Microtubule-Associated Protein AtMPB2C Plays a Role in Organization of Cortical Microtubules, Stomata Patterning, and Tobamovirus Infectivity[1]

Pia Ruggenthaler, Daniela Fichtenbauer, Julia Krasensky, Claudia Jonak, and Elisabeth Waigmann*

Max F. Perutz Laboratories, University Departments at the Vienna Biocenter, Department of Medical Biochemistry, Medical University of Vienna, 1030 Vienna, Austria (P.R., D.F., E.W.); and Gregor Mendel Institute of Molecular Plant Biology, Austrian Academy of Sciences, 1030 Vienna, Austria (J.K., C.J.)

AtMPB2C is the Arabidopsis (*Arabidopsis thaliana*) homolog of MPB2C, a microtubule-associated host factor of tobacco mosaic virus movement protein that was been previously identified in *Nicotiana tabacum*. To analyze the endogenous function of AtMPB2C and its role in viral infections, transgenic Arabidopsis plant lines stably overexpressing green fluorescent protein (GFP)-AtMPB2C were established. The GFP-AtMPB2C fusion protein was detectable in various cell types and organs and localized at microtubules in a punctuate pattern or in filaments. To determine whether overexpression impacted on the cortical microtubular cytoskeleton, GFP-AtMPB2C-overexpressing plants were compared to known microtubular marker lines. In rapidly elongated cell types such as vein cells and root cells, GFP-AtMPB2C overexpression caused highly unordered assemblies of cortical microtubules, a disturbed, snake-like microtubular shape, and star-like crossing points of microtubules. Phenotypically, GFP-AtMPB2C transgenic plants showed retarded growth but were viable and fertile. Seedlings of GFP-AtMPB2C transgenic plants were characterized by clockwise twisted leaves, clustered stomata, and enhanced drought tolerance. GFP-AtMPB2C-overexpressing plants showed increased resistance against *Oilseed rape mosaic virus*, a close relative of *Tobacco mosaic virus*, but not against *Cucumber mosaic virus* when compared to Arabidopsis wild-type plants. These results suggest that AtMPB2C is involved in the alignment of cortical microtubules, the patterning of stomata, and restricting tobamoviral infections.

Spread of the viral RNA genome of *Tobacco mosaic virus* (TMV) between plant cells is mediated by a virus-encoded movement protein (TMV-MP). Binding of TMV-MP to the folded viral RNA leads to unfolding of viral RNA and mediates the transport of RNA/TMV-MP complexes through plasmodesmata into neighboring plant cells. To facilitate transfer, TMV-MP is thought to increase the size exclusion limit of plasmodesmata. Typically, TMV-MP shows three characteristic subcellular localization patterns: punctae associated with the endoplasmic reticulum, filamentous structures identified as microtubular localization, and cell wall-associated punctae representing plasmodesmatal localization. Based on these patterns, it was suggested that viral RNA/TMV-MP complexes are likely formed in the neighborhood of the endoplasmic reticulum and then transported to plasmodesmata via microtubules (for review, see Heinlein, 2002; Waigmann et al., 2004; Lucas, 2006; Hofmann et al., 2007). The role of microtubules in this process is controversial, and an alternative transport route via the ER/actin network has been proposed (Liu et al., 2005; Wright et al., 2007).

To gain further insight into the transport process, TMV-MP-interacting host factor MPB2C was identified in *Nicotiana tabacum* and analyzed. Endogenous MPB2C localized in punctae at cortical microtubules, suggesting its interaction with distinct sites at microtubules (Kragler et al., 2003). The localization of MPB2C at microtubules suggests that MPB2C belongs to the group of microtubule-associated proteins (MAPs; Sedbrook, 2004; Wasteneys, 2004) thought to mediate the versatility and architecture of diverse microtubular assemblies. Upon transient overexpression in *N. tabacum* leaves, MPB2C mediated subcellular redistribution of TMV-MP from plasmodesmata toward microtubules and the endoplasmic reticulum, thereby interfering with the cell-to-cell transport activity of TMV-MP (Kragler et al., 2003). Virus-induced gene silencing of MPB2C led to a loss of microtubular localization of TMV-MP, but no change in local or systemic viral spread was observed. Taken together, these results indicate that MPB2C mediates efficient accumulation of TMV-MP at microtubules. However this accumulation is not required for cell-to-cell transport (Curin et al., 2007). Potentially, the suggested

[1] This work was supported by Austrian Science Foundation (Sfb17 project part 08 to E.W. and P20375–B03 to C.J.), by Wiener Wissenschafts-, Forschungs- und Technologiefonds (project LS123 to C.J. and E.W.), and by Austrian Agency for International Cooperation in Education and Research (project 18/2006 to E.W.).

* Corresponding author; e-mail elisabeth.waigmann@meduniwien.ac.at.

The author responsible for the distribution of materials integral to the findings presented in this article in accordance with the policy described in the Instructions for Authors (www.plantphysiol.org) is: Elisabeth Waigmann (elisabeth.waigmann@meduniwien.ac.at).

www.plantphysiol.org/cgi/doi/10.1104/pp.108.130450

microtubule-associated transport pathway for viral RNA/TMV-MP complexes toward plasmodesmata might be relevant during early stages of TMV infection (Waigmann et al., 2004; Boyko et al., 2007), whereas at later stages in infection, when the virus replicates and forms virions, MPB2C-mediated accumulation of TMV-MP at microtubules could be a strategy to inactivate the transport function of TMV-MP (Waigmann et al., 2004; Boyko et al., 2007).

Recently, colocalization and interaction between TMV-MP and GFP-tagged microtubule end binding protein AtEB1 has been reported. Transient overexpression of AtEB1:GFP following agroinfiltration correlated to a reduction of cell-to-cell spread in *Nicotiana benthamiana* of a TMV derivative expressing an MP:RFP fusion protein (Brandner et al., 2008). Potentially, MPB2C and AtEB1:GFP might share a role in regulating TMV-MP transport function.

The endogenous function of MPB2C is not fully explored yet. Recently, it was demonstrated that cell-to-cell transport of KNOTTED1, a transcription factor, was inhibited upon interaction with MPB2C (Winter et al., 2007). MPB2C might mediate targeting of KNOTTED1 to microtubules that might eventually lead to degradation, thereby regulating KNOTTED1 function in the shoot apical meristem (Winter et al., 2007).

To further characterize the MPB2C's endogenous function, AtMPB2C, the single Arabidopsis (*Arabidopsis thaliana*) homolog of MPB2C, was stably overexpressed as a GFP-AtMPB2C fusion protein in Arabidopsis plants. Cortical microtubular assemblies and the overall phenotype were analyzed. A striking phenotype characterized by clockwise twisted leaves and clustered stomata was observed. GFP-AtMPB2C transgenic plants were also used to study the effect of overexpressed AtMPB2C on viral spread. Because Arabidopsis is not an ideal host for TMV, the closely related tobamovirus *Oilseed rape mosaic virus* (ORMV; Aguilar et al., 1996) as well as *Cucumber mosaic virus* (CMV; Roossinck et al., 1999) were used to infect Arabidopsis plants. GFP-AtMPB2C-overexpressing plants showed increased resistance against ORMV infection, but not against CMV infection, indicating that AtMPB2C is a negative regulator of ORMV infection and that this regulation is specific for ORMV.

RESULTS

Alignment of MPB2C Proteins

Arabidopsis contains only a single homolog of MPB2C, AtMPB2C, with a calculated molecular mass of 37,35 kD (Kragler et al., 2003; Winter et al., 2007). Thus, Arabidopsis presents an ideal system to study the function of the AtMPB2C protein. Bioinformatic analysis of NtMPB2C, NbMPB2C, and AtMPB2C highlights a coiled-coil region (Lupas et al., 1991) in AtMPB2C similar as described for the *N. tabacum* MPB2C (Kragler et al., 2003). An alignment of MPB2C protein sequences from Arabidopsis, *N. tabacum*, and *N. benthamiana* showed four conserved domains (Fig. 1), with domain II and III located within the coiled-coil region. Thus, there is considerable similarity, suggesting that AtMPB2C has functions similar to the NtMPB2C and NbMPB2C proteins.

Generation of GFP-AtMPB2C-Overexpressing Arabidopsis Plants

To further characterize AtMPB2C functions, the generation of AtMPB2C knockdown plants and GFP-AtMPB2C overexpression lines was attempted, the latter one with the aim to facilitate microtubular analysis on the subcellular level. Whereas in the case of knockdown lines, whose generation was attempted by transforming plants with a silencing construct, no transformants could be regenerated (data not shown), the generation of GFP-AtMPB2C overexpression lines was successful. AtMPB2C cDNA was cloned by reverse transcription-PCR from RNA derived from Arabidopsis ecotype Columbia (Col-0) into the binary vector pMDC43, an overexpression vector, which contains two 35S cauliflower mosaic virus promoters followed by the GFP coding sequence (Curtis and Grossniklaus, 2003) to enable expression of GFP-AtMPB2C fusion protein at high levels. Arabidopsis wild-type plants were transformed by Agrobacterium-mediated transformation (Clough and Bent, 1998) and several nonsegregating transgenic lines were established. To confirm overexpression of GFP-AtMPB2C in those lines, total protein extracts were analyzed by western blotting with a GFP antibody. Indeed, in GFP-AtMPB2C transgenic plants, a band at the expected height of the GFP-AtMPB2C fusion protein was present, which was absent in wild-type plants (Fig. 2, compare lanes 2 and 3 to lane 1). Two lines were selected for subsequent experiments and yielded similar results.

GFP-AtMPB2C Localizes to and Stabilizes Microtubules

Previous experiments in *N. tabacum* indicated punctuate localization of MPB2C at microtubules (Kragler et al., 2003). To test whether AtMPB2C was similarly localized, its subcellular localization in Arabidopsis was evaluated in two ways. Firstly, by transient expression of GFP-AtMPB2C via biolistic delivery into wild-type plants and secondly by analyzing various cell types in transgenic plants expressing GFP-AtMPB2C.

For transient expression, the pMDC43-GFP-AtMPB2C vector was biolistically delivered into epidermal leaf cells of Arabidopsis Col-0 wild-type plants. Expressing cells were analyzed by confocal microscopy. The GFP-AtMPB2C fusion protein showed a punctuate localization pattern (Fig. 3A). In transgenic Arabidopsis plants, GFP-AtMPB2C fusion protein was clearly detectable in various tissues and

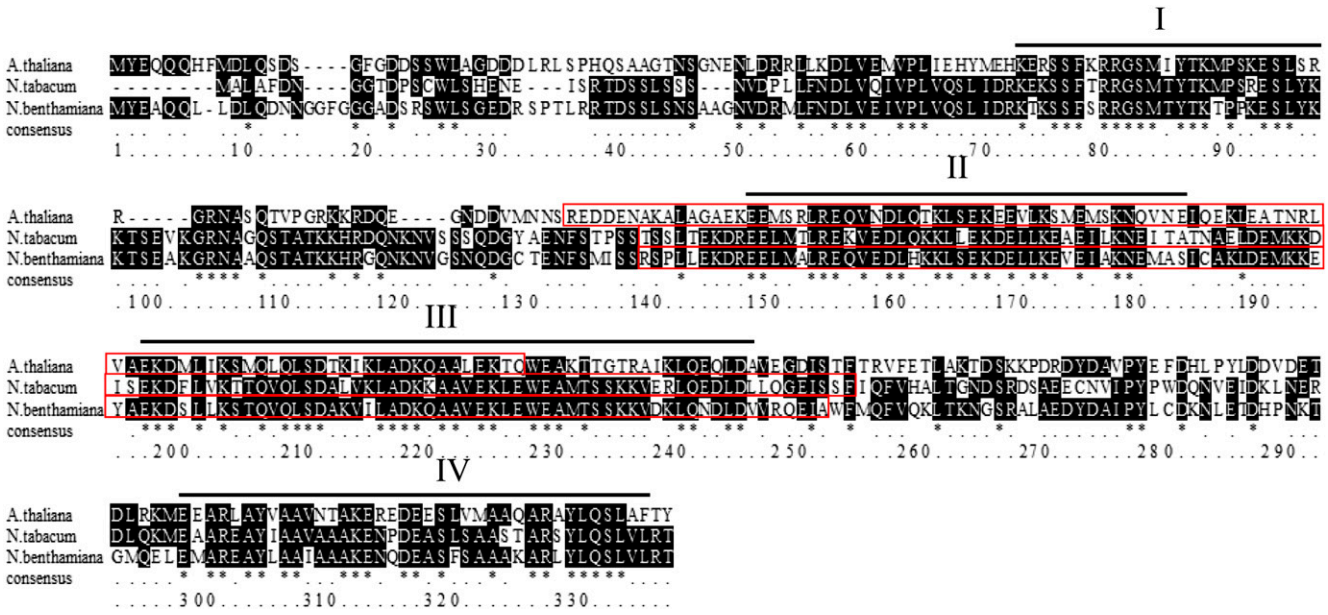

Figure 1. Alignment and sequence analysis of AtMPB2C, NtMPB2C, and NbMPB2C protein sequences. The NtMPB2C and NbMPB2C sequences were deposited in GenBank accession nos. AF326729 and DQ297413. AtMPB2C sequence accession no. At5g08120 was found at The Arabidopsis Information Resource (http://www.arabidopsis.org/index.jsp). Black shading represents identical amino acids, * represents identical amino acids in all three proteins, **.** indicates identical amino acids in only two protein sequences, black lines indicate conserved regions (I–IV), and red boxes indicate coiled coil domains.

organs by confocal microscopy. In epidermal leaf cells, GFP-AtMPB2C appeared either as a mixture of filaments and punctae (Fig. 3B) or it localized solely in filaments (Fig. 3C).

Punctuate localization of AtMPB2C was similar to the pattern observed for endogenous MPB2C detected in *N. tabacum* protoplasts (Kragler et al., 2003). Filamentous localization pattern was also previously observed for an N terminally truncated version of MPB2C, which decorated microtubules in a continuous fashion (Kragler et al., 2003). In the case of GFP-AtMPB2C overexpression lines, filamentous appearance is probably due to the high levels of protein. In summary, AtMPB2C displays a localization pattern in line with the pattern found for the tobacco homolog, indicating that AtMPB2C likely localizes to microtubules.

To confirm that GFP-AtMPB2C binds to microtubules, plant leaves were treated with oryzalin, a drug that inhibits polymerization of microtubules (Hugdahl and Morejohn, 1993). As a control, a GFP-TUA6 line (Ueda et al., 1999) was used, where α-tubulin fused to GFP is overexpressed and readily incorporated into microtubules. Leaves of GFP-AtMPB2C overexpression lines and of control plants were incubated in 20 μM oryzalin in 0.1% ethanol or in 0.1% ethanol for 20 h. Confocal images were taken before and at the end of the incubation period. GFP-AtMPB2C appeared in filaments before treatment (Fig. 3D) and after 20-h incubation in 0.1% ethanol (Fig. 3E). After incubation in 20 μM oryzalin, filaments disappeared and a uniform cytoplasmic fluorescence was observed instead (Fig. 3F). GFP-TUA6-expressing leaves showed fluorescent filaments representing microtubules before treatment (Fig. 3G; Ueda et al., 1999). After 20 h of treatment with 20 μM oryzalin, GFP-TUA6 appeared as diffuse cytoplasmic labeling, indicating that microtubules were depolymerized (Fig. 3I). Interestingly, incubation in 0.1% ethanol resulted already in a strong reduction of filamentous labeling, as only occasionally was labeling of microtubules visible (Fig. 3H, arrows).

Overall, these results indicate that GFP-AtMPB2C localizes to microtubules. However, in contrast to GFP-TUA6, GFP-AtMPB2C likely exerts a stabilizing function, because microtubules remained intact upon incubation in ethanol (Fig. 3E), whereas GFP-TUA6-labeled microtubules were largely lost under those conditions (Fig. 3H).

GFP-AtMPB2C Interferes with Cortical Microtubular Assemblies

To determine if overexpression of GFP-AtMPB2C changes the organization of the cortical microtubular cytoskeleton, GFP-AtMPB2C-overexpressing plants were compared to known microtubular marker lines expressing MAP4-GFP and GFP-TUA6. In the MAP4-GFP transgenic line, MAP4 is overexpressed in Arabidopsis ecotype Col-0 and decorates microtubules (Marc et al., 1998; Granger and Cyr, 2001).

Cortical microtubular assemblies showed a striking difference between GFP-AtMPB2C-overexpressing

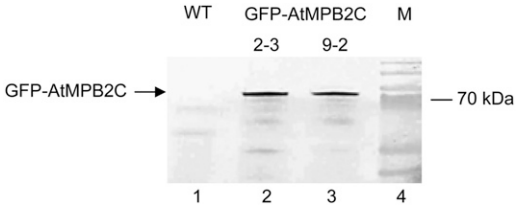

Figure 2. Analysis of GFP-AtMPB2C overexpression in extracts derived from total plants by western blotting with anti-GFP antibody (lane 1, wild-type [WT] plant; lane 2, GFP-AtMPB2C plant 2–3; lane 3, GFP-AtMPB2C plant 9–2; lane 4, size marker [M]). Arrow indicates overexpressed GFP-AtMPB2C.

lines and marker lines in vein cells and roots. In GFP-AtMPB2C-overexpressing trichomes, vein cells and root cells microtubules appeared snake-like (Fig. 4, A, C, E, and F, arrows) and crossed each other, forming star-like clusters (Olson et al., 1995; Fig. 4, A, C, E, and F, circles). This was in contrast to the marker lines, where microtubules in those cell types had a more straight shape (Fig. 4, B, D, and G). The regularity of cortical microtubular arrays in vein cells and root cells also differed between GFP-AtMPB2C-overexpressing transgenic plants (Fig. 4, E and F) and those in the marker lines (Fig. 4G). GFP-AtMPB2C-decorated microtubules were unordered and extended in all directions (Fig. 4, C, E, and F). In contrast, microtubules in control root cells and vein cells were regularly ordered and arrayed transversely to the longitudinal axis (Fig. 4, D and G) similar to cortical microtubular arrays in Arabidopsis wild-type plants (Abe and Hashimoto, 2005). Interestingly, in cells where GFP-AtMPB2C manifested as punctae, enrichment at some microtubular star-like clusters became apparent (Fig. 4E, orange circles).

Furthermore, analysis of the cortical microtubular array in root tips was performed. GFP-AtMPB2C-decorated microtubules showed strong bundling, leading to short and thick microtubules (Fig. 4H). In root tips of MAP4-GFP-overexpressing plants, however, no bundling of microtubules was observed (Fig. 4I).

In summary, overexpression of GFP-AtMPB2C leads to severe disturbance of cortical microtubular arrays in elongated cell types such as trichomes, vein cells, and root cells, as well as in root tips.

GFP-AtMPB2C-Overexpressing Plants Are Characterized by Clockwise Twisted Leaves

Transgenic plants overexpressing GFP-AtMPB2C showed retarded growth and reduced efficiency in the production of seeds but were viable and fertile (data not shown). Interestingly, seedlings grown on GM medium or soil developed clockwise twisted leaves. On GM medium, this phenotype first became apparent in 13-d-old seedlings and became more pronounced during development (Fig. 5A, left); it was clearly absent from wild-type seedlings grown in the same conditions (Fig. 5B, right). The phenotype was also visible in older plants grown directly on soil (Fig. 5B, left). Because leaves were twisted, we also examined petioles to see whether any differences in cellular arrangement were apparent. Petioles of GFP-

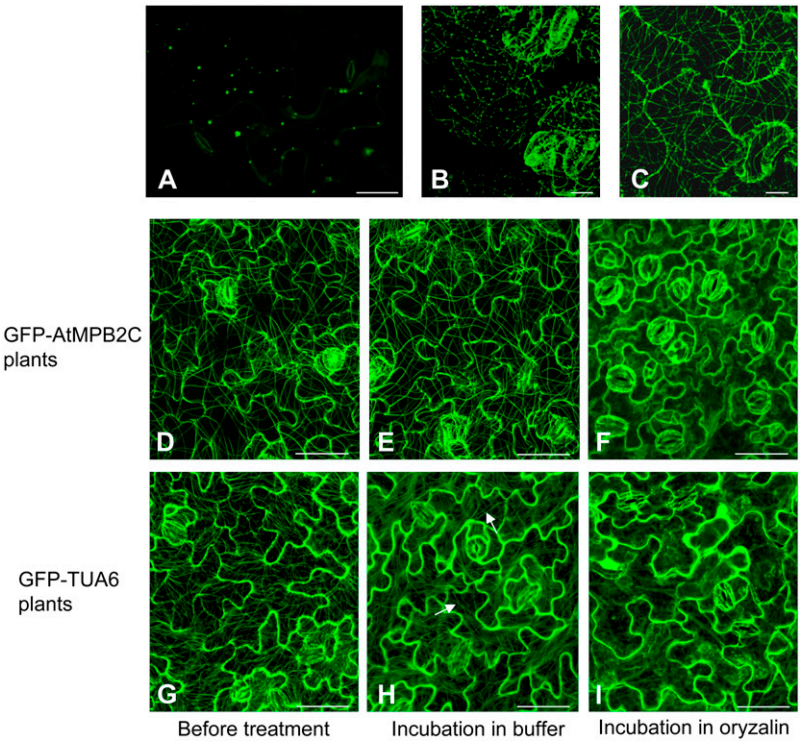

Figure 3. Localization of GFP-AtMPB2C at microtubules in epidermal leaf cells. A, Transient overexpression of a binary vector expressing GFP-AtMPB2C in epidermal leaf cells of Arabidopsis Col-0. GFP-AtMPB2C localizes at puncta. B and C, Epidermal leaf cells stably overexpressing GFP-AtMPB2C. Punctate pattern (B) and continuous decoration of microtubules visible (B and C). Transgenic plants treated with oryzalin. D, GFP-AtMPB2C epidermal cells before treatment. E, GFP-AtMPB2C epidermal cells after overnight incubation in buffer. F, GFP-AtMPB2C epidermal cells after overnight incubation in 20 μM oryzalin. G, GFP-TUA6 epidermal cells before treatment. H, GFP-TUA6 epidermal cells after overnight incubation in buffer. Arrows point to microtubular filaments. I, GFP-TUA6 epidermal cells after overnight incubation in 20 μM oryzalin. Bar in A to C = 10 μm; D to I = 40 μm.

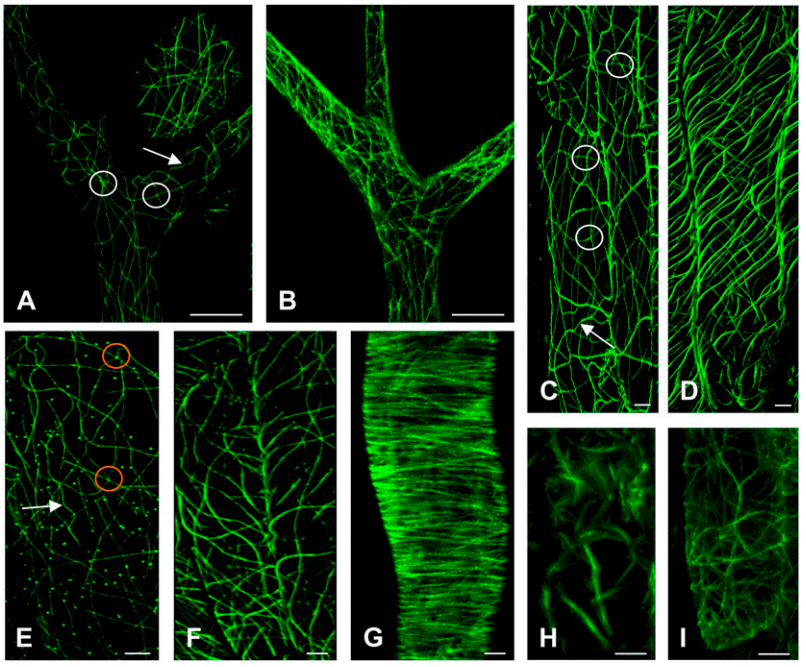

Figure 4. A, Overexpression of GFP-AtMPB2C in trichomes. The microtubular cytoskeleton appears unordered and microtubules are snake-like (arrow), circles indicate star-like clusters. B, Overexpression of MAP4-GFP in trichomes. C, GFP-AtMPB2C overexpressed in vein cells. The microtubular array is unordered, microtubules are snake-like (arrow), and microtubules cross each other. Circles indicate crossing points. D, MAP4-GFP overexpressed in vein cells. Microtubules are parallel oriented to each other. E and F, GFP-AtMPB2C stably overexpressed in roots. The microtubular array appears unordered, the microtubules are snake-like (arrow) and cross each other; at crossing points of microtubules, GFP-AtMPB2C is enriched. Orange circles indicate enrichment of GFP-AtMPB2C. G, GFP-TUA6 overexpressed in roots. The microtubules are straight and transverse oriented. H, GFP-AtMPB2C overexpressed in root tips. GFP-AtMPB2C labeling of microtubules leads to a strong bundling of microtubules. I, MAP4-GFP overexpressed in root tips. Bar in A, B, H, and I = 40 μm; C to G = 10 μm.

AtMPB2C-overexpressing plants appeared thicker than those of wild-type plants (Fig. 5A, bottom). At the microscopic level, this impression was clearly confirmed (Fig. 5C). Here, individual cells of the petioles were larger in GFP-AtMPB2C-expressing lines than in their wild-type counterparts. However epidermal cells were arranged in regular files oriented along the axis of the petiole (Fig. 5C), both in GFP-AtMPB2C-expressing lines and in wild-type plants, indicating that arrangement of epidermal cell files is not the cause for the twisted leaf phenotype.

GFP-AtMPB2C-Overexpressing Plants Show Disturbed Stomata Patterning

MPB2C has been identified as a negative regulator of viral cell-to-cell transport (Kragler et al., 2003; Curin et al., 2007). Therefore, it was hypothesized that on the endogenous level, MPB2C functions might include regulation of endogenous non-cell-autonomous processes. One of those processes is the patterning of stomata at leaf surfaces. Stomata are almost always separated from each other by at least one intervening

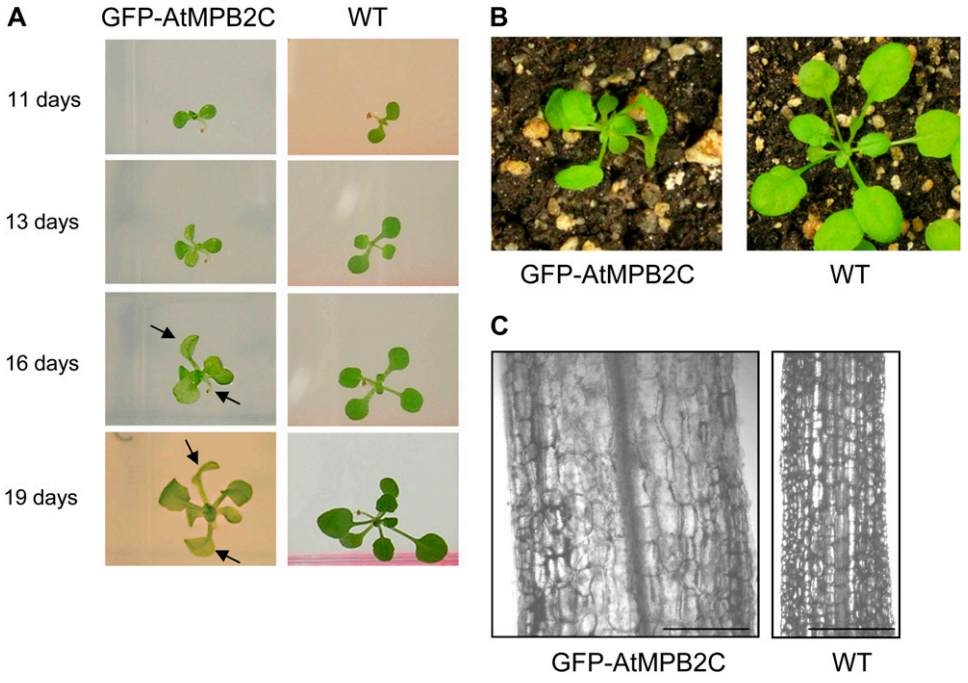

Figure 5. A, GFP-AtMPB2C-overexpressing plants grown on GM medium show clockwise twisting of leaves (left; arrows point to clockwise twisted leaves). Wild-type (WT) plants do not show this phenotype (right). B, GFP-AtMPB2C-overexpressing plants grown on soil also show clockwise twisting of leaves (left) when compared to WT plants (right). C, Petioles of GFP-AtMPB2C are thicker than petioles of WT plants. Bars in C = 1 mm.

cell (Bergmann and Sack, 2007). This phenomenon is also called the one-cell-spacing rule.

When the abaxial side of leaves of GFP-AtMPB2C transgenic plants grown on GM medium was examined, two or more stomata located next to each other could frequently be observed (Fig. 6, A and B). In contrast, in Arabidopsis wild-type plants. stomata were usually separated by at least one cell (Fig. 6C). To quantify this phenomenon, stomata of 12 leaves from GFP-AtMPB2C-overexpressing plants and wild-type plants were evaluated. In GFP-AtMPB2C-overexpressing lines, 75% of stomata were single, 18.5% were paired, 5.4% were triples, and 1% of stomata were found even in quartettes (Fig. 6D). Stomata in clusters were positioned at various angles to each other (compare, for example, stomata in box in Fig. 6A and in top box in Fig. 6B). In Arabidopsis wild-type plants, most of the stomata (96.1%) were single and only 3.9% were paired. No triple or quartette stomata were observed (Fig. 6E). Individual stomata appeared similar in GFP-AtMPB2C-overexpressing plants and wild-type plants; they showed bilateral symmetry and were always composed of paired cells. In addition, the number of stomatal units (SU), the number of separate stomatal sites (Yang and Sack, 1995), increased from 125 SU/mm^2 in wild type to 247 SU/mm^2 in GFP-AtMPB2C overexpression plants, indicating that stomatal sites are denser and the absolute number of stomata is larger in GFP-AtMPB2C overexpression plants. In summary, this analysis suggests that in GFP-AtMPB2C-overexpressing plants, the morphology of individual stomata is retained, whereas stomata patterning is severely disturbed.

Overexpression of AtMPB2C Increases Resistance against Drought Stress

Stomata control water loss under changing environmental conditions. Prompted by the increased number of stomata in plants overexpressing AtMPB2C, we analyzed the performance of these plants under drought stress conditions. Four-week-old, soil-grown, wild-type plants and overexpressor line GFP-AtMPB2C were exposed to a severe drought and analyzed for their survival rate. After a period of withholding water for 14 d, GFP-AtMPB2C-overexpressing plants showed significantly less wilting than wild-type plants. After rehydration for 48 h, 70% of GFP-AtMPB2C plants had recovered, while all wild-type plants had died (Fig. 7), showing that AtMPB2C overexpressors tolerate severe drought periods significantly better than wild-type plants.

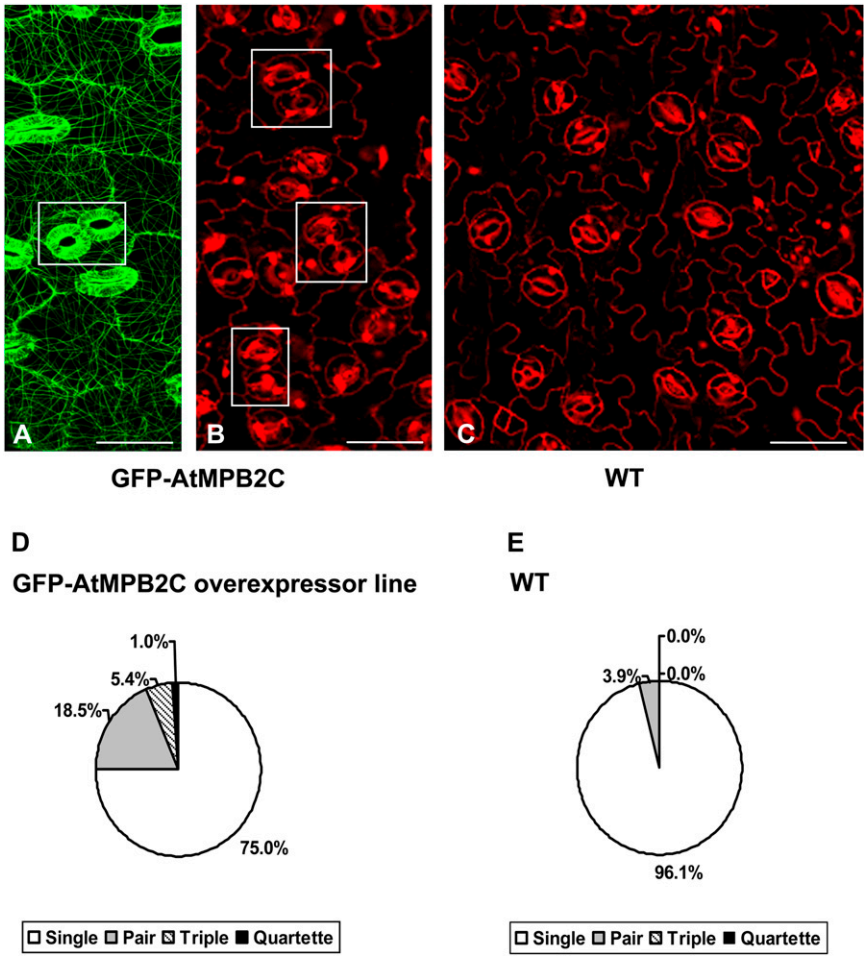

Figure 6. Microscopic evaluation of stomata patterning in GFP-AtMPB2C-overexpressing and wild-type (WT) plants. A and B, GFP-AtMPB2C-overexpressing plants grown on GM medium show clusters of paired stomata (white boxes indicate clustered stomata). C, Regular stomata patterning in WT plants grown on GM medium. Plant material in B and C is stained with propidium iodide. Bars = 40 μm. D, Quantitative distribution of stomata in GFP-AtMPB2C-overexpressing plants. E, Quantitative distribution of stomata in WT plants.

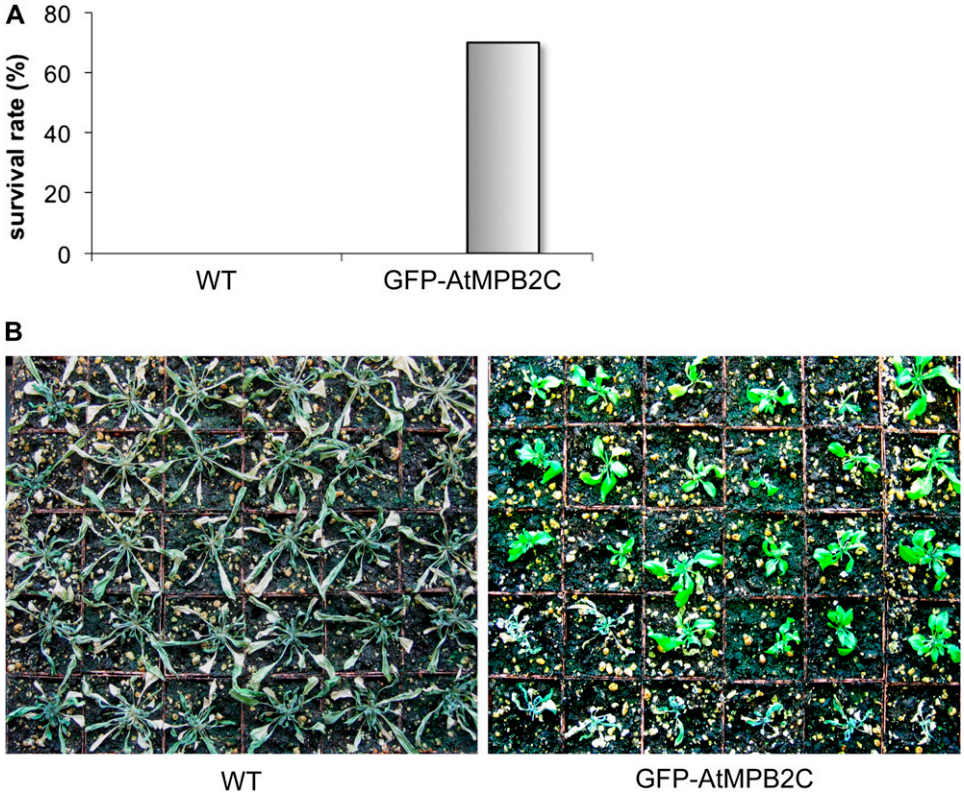

Figure 7. Increased drought tolerance of GFP-AtMPB2C-overexpressor plants. Thirty plants of Arabidopsis wild type (WT) and GFP-AtMPB2C overexpressor line were grown in soil for 4 weeks. Drought was implemented by withholding water for 14 d. Survival rate was evaluated 48 h after rewatering of the plants. A, Quantification of survival rate. B, Plants were randomly distributed during stress treatment and were arranged afterward for taking pictures.

GFP-AtMPB2C-Overexpressing Plants Show Increased Resistance against ORMV Infection

Based on the known negative effect of transiently overexpressed MPB2C on TMV-MP cell-to-cell movement in *N. tabacum* (Kragler et al., 2003), it was expected that stable overexpression of AtMPB2C in plants might have a negative effect on TMV infections. Due to the symptomless nature of TMV infection in Arabidopsis (Martín et al., 1997), we used a related tobamovirus, ORMV, to test this hypothesis with the GFP-AtMPB2C-overexpressing lines.

A total of 120 GFP-AtMPB2C-overexpressing plants and 120 Arabidopsis wild-type plants were inoculated with ORMV. To evaluate whether plants were infected or not, total protein extracts were analyzed for the presence of viral coat protein, which is made in large amounts during tobamovirus infection and can be easily detected (Curin et al., 2007). Indeed, a band at the expected height of the ORMV coat protein could be clearly detected 14 d after inoculation (Fig. 8A, compare lanes 2 and 3). At 3, 5, 7, and 14 d after inoculation, plants were harvested and their infection status was determined. For wild-type plants, none were infected at 3 d postinoculation (DPI), 63.3% of plants were infected at 5 DPI, 76.7% at 7 DPI, and 90% of plants were infected at 14 DPI (Fig. 8B). For GFP-AtMPB2C-overexpressing plants, none were infected at 3 DPI, 30% at 5 DPI, 36.7% at 7 DPI, and 53.3% of GFP-AtMPB2C-overexpressing plants were infected at 14 DPI (Fig. 8B). These results indicate that overexpression of GFP-AtMPB2C has a negative effect on ORMV infections and that plants overexpressing GFP-AtMPB2C show increased resistance against ORMV.

To determine whether increased resistance is specific for ORMV infections or a more general effect, the LS strain of CMV (LS-CMV) was employed for a similar study. Again, detection of coat protein was used to determine the infection status of a plant (Fig. 8C). At 3 DPI, neither Arabidopsis wild-type plants nor GFP-AtMPB2C-overexpressing plants were infected. At 7 DPI, 6.3% of wild-type plants were infected, 27.3% at 10 DPI, and 25% at 14 DPI of wild-type plants were infected (Fig. 8D). At 7 DPI 9.4% of GFP-AtMPB2C-overexpressing plants were infected, 31.6% at 10 DPI, and 31.3% at 14 DPI (Fig. 8D). Thus, GFP-AtMPB2C-overexpressing plants and Arabidopsis wild-type plants do not show a significant difference in infectivity, indicating that overexpression of GFP-AtMPB2C has no effect on LS-CMV infection.

Taken together, these results confirm the hypothesis that stable overexpression of AtMPB2C in plants has a negative effect on ORMV infections. This negative effect is likely specific for ORMV infections, because LS-CMV infections were not impaired.

DISCUSSION

Previous studies in *N. tabacum* and *N. benthamiana* have identified the MPB2C protein as a MAP that acts

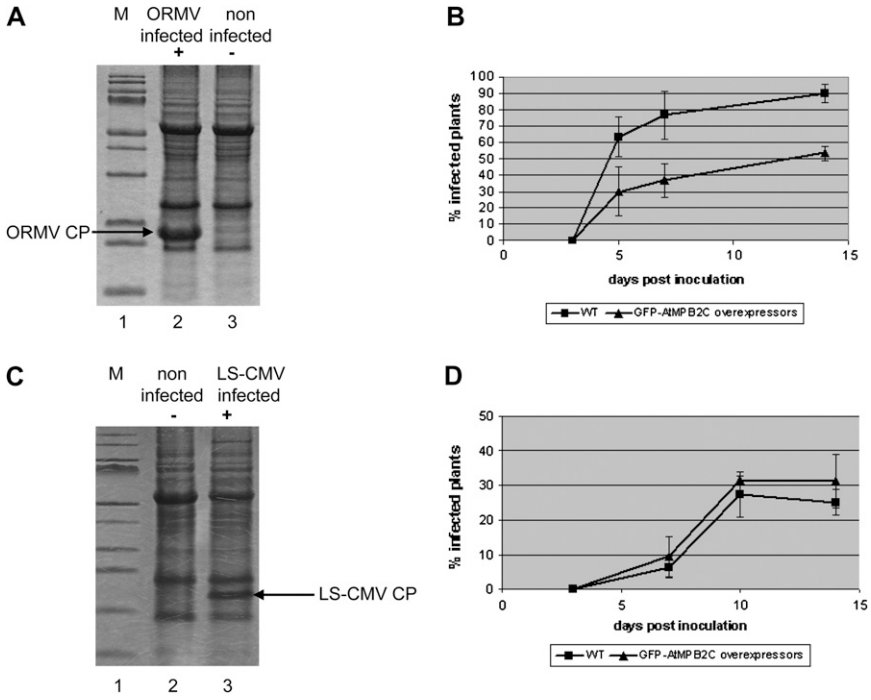

Figure 8. Differences in infectivity of GFP-AtMPB2C-overexpressing and wild-type (WT) plants. A, Coat protein (CP) assay. Viral infection was assayed by detection of ORMV CP lane 1, size marker (M); lane 2, protein extract of ORMV-infected Arabidopsis plant 14 d postinoculation; lane 3, protein extract of noninfected Arabidopsis plant). Arrow indicates ORMV coat protein (17 kD). B, Time course of infectivity. GFP-AtMPB2C-overexpressing plants show increased resistance when compared to Arabidopsis WT plants. C, CP assay. Viral infection was assayed by detection of 24-kD LS-CMV CP (lane 1, size marker; lane 2, protein extract of noninfected Arabidopsis plant; lane 3, protein extract of LS-CMV-infected Arabidopsis plant 14 d postinoculation). Arrow indicates LS-CMV CP. D, Time course of infectivity. LS-CMV-infected GFP-AtMPB2C-overexpressing plants show similar infection rate as infected Arabidopsis WT plants.

as a negative regulator of TMV-MP cell-to-cell movement (Kragler et al., 2003; Curin et al., 2007). Also, the single MPB2C homolog in Arabidopsis, AtMPB2C, was recently found to exert a negative effect on cell-to-cell movement of KNOTTED1 and SHOOTMERISTEMLESS upon transient expression (Winter et al., 2007). However, a more complete picture of AtMPB2C function, in particular with regard to its role in microtubular assemblies, plant development, and viral infections, is still lacking. To bridge this gap, we initially attempted to generate AtMPB2C knock down lines. However, this endeavor failed. An explanation might be that AtMPB2C is potentially an essential factor for plant development, and thus knockdown/knockout plants cannot be regenerated. Inline, AtMPB2C was reported to be constitutively expressed in seedlings (Winter et al., 2007). The function of plant MAPs has been frequently studied in plants mutant in (Whittington et al., 2001; Thitamadee et al., 2002) or overexpressing the particular MAP (Ambrose et al., 2007; Korolev et al., 2007). Therefore, we switched our strategy and established Arabidopsis plants stably overexpressing a N-terminal fusion between GFP and AtMPB2C (GFP-AtMPB2C).

First, the localization pattern of GFP-AtMPB2C overexpressed in transgenic lines was analyzed in different organs and tissues by confocal microscopy, such as epidermal cells in rosette leaves, trichomes, vein cells, and root cells. A clear signal derived from GFP-AtMPB2C was detected, which appeared mostly in filaments. Additionally, in some cells a punctuate localization of GFP-AtMPB2C was visible, similar to the known pattern of endogenous NtMPB2C, which localizes in puncta at microtubules (Kragler et al., 2003). Thus, the filaments and puncta decorated by GFP-AtMPB2C suggest microtubular localization of the fusion protein, with puncta most likely reflecting the endogenous localization of AtMPB2C, whereas continuous decoration of microtubules by GFP-AtMB2C might be a consequence of overexpression. A similar effect was observed previously for CLIP-170, a protein that also localizes in punctae at microtubules but shows continuous labeling of microtubules when overexpressed (Pierre et al., 1994). The same two localization patterns, puncta and filaments, were observed for transiently expressed C-terminal fusions of AtMPB2C to fluorescent tags in *N. benthamiana* leaves (Winter et al., 2007), indicating that neither the position of the tag nor the plant background influences the localization of the AtMPB2C protein.

The suspected microtubular localization of GFP-AtMPB2C was confirmed by incubation of leaves with the microtubule-depolymerizing drug oryzalin, which led to a loss of filamentous fluorescence. Interestingly, GFP-AtMPB2C-labeled microtubules were more resistant against depolymerization than microtubules labeled with GFP-TUA6, indicating that GFP-AtMPB2C stabilizes microtubules. A microtubule-stabilizing function has also been reported for other MAPs such as CLASP1 (Ambrose et al., 2007) and AtMAP70-5 (Korolev et al., 2007). Interestingly, TMV-MP, whose microtubular localization in plants is mediated by the Nicotiana homolog of MPB2C (Curin et al., 2007), also exerts a microtubule-stabilizing function (Ashby et al., 2006).

Transgenic plants overexpressing GFP-AtMPB2C exhibited severe loss of regularity in cortical microtubular arrays in rapidly elongating cells, such as vein cells and root cells, where microtubules of cortical arrays are highly ordered in wild-type plants (Granger

and Cyr, 2001). There, cortical microtubules showed a snake-like appearance and were oriented in various directions, frequently crossing each other. In root tips of GFP-AtMPB2C-overexpressing plants, pronounced bundling was observed, giving rise to short and thick microtubules. Even though several other MAPs such as CLASP1, SPR2, AtMAP70-5, and MOR1 (Whittington et al., 2001; Shoji et al., 2004; Kawamura et al., 2006; Ambrose et al., 2007; Korolev et al., 2007) have been overexpressed as GFP fusion proteins in Arabidopsis, none of these proteins was reported to exert a similar dramatic effect on the organization of cortical microtubules. Our observations suggest that the overexpression of GFP-AtMPB2C interferes with proper function of endogenous AtMPB2C. (The endogenous function of AtMPB2C might be linked to alignment of cortical microtubules.)

A second strong phenotype associated with GFP-AtMPB2C-overexpressing seedlings was the clockwise twisting of leaves. On a microscopic level, petioles of GFP-AtMPB2C-overexpressing plants were thicker and contained larger cells than those of wild-type plants, but cells were arranged in regular files oriented along the axis of the petiole.

Twisting of leaves is a known phenomenon in plant science frequently associated with MAPs or tubulin mutants. For example, in *spr2* plants mutated in the MAP SPIRAL2, right handed-helical growth of the epidermal cells of petioles apparently causes counterclockwise arrangement of cotyledons and rosette leaves (Buschmann et al., 2004; Shoji et al., 2004). The underlying cause is provided by reduced anisotropic growth of ground tissue cells in spiral mutants, which led to shorter total longitudinal length compared to that of epidermal cells. To compensate for this difference, epidermal cell files had to twist, thus accounting for the observed twisted leaf phenotype (Hashimoto, 2002). Mutants in other MAPS such as *mor1* and *wave-dampened2-1* (*wvd2-1*), as well as plants overexpressing MAPs AtMAP70-5 and WVD2 showed twisted organs, indicating that compromised growth anisotropy is a frequent phenomenon caused by lack of or excessive amounts of MAPs (Whittington et al., 2001; Yuen et al., 2003; Korolev et al., 2007). Not only MAPs but also a collection of mutants in α and β tubulins (Thitamadee et al., 2002; Ishida et al., 2007) and plants overexpressing GFP-TUA6 (Abe and Hashimoto, 2005) showed either right-or left-handed helical growth of epidermal cells of petioles, resulting in twisting of cotyledons and leaves.

Taken together, the clockwise twisting leaf phenotype of GFP-AtMPB2C-overexpressing plants is in line with previously observed twisting of organs in plants mutant or overexpressing MAPs. Remarkable, however, is the observation that GFP-AtMPB2C-overexpressing plants do not display helical growth in epidermal cell files of petioles, indicating that the twisting leaf phenotype is likely generated by a different mechanism.

Another phenotypic effect in plants overexpressing GFP-AtMPB2C is the clustering of stomata, which was observed on the abaxial side of leaves when plants were grown on GM medium. A total of 75% of stomata were single and surrounded by a stoma-free region, whereas 25% were in clusters of two or more stomata. Additionally, the number of stomata and SU/mm^2 was increased in GFP-AtMPB2C-overexpressing plants as compared to wild-type Arabidopsis. A clustered stomata phenotype has been described for several other Arabidopsis mutants that fall into two distinct groups (for review, see Bergmann and Sack, 2007). One group shows stomata clusters that consist only of paired guard cells arranged in various angles to each other. For example, the *too many mouth* (*tmm*) mutant (Yang and Sack, 1995), *stomatal density and distribution1* (*sdd1*; Von Groll et al., 2002), a triple mutant of *erecta* (*er*), *erecta-like1* (*erl1*) and *erl2*, and the mutant *yoda* (Bergmann, 2004; Shpak et al., 2005) belong to this group. The second group consists of mutants that show not only clusters composed of paired guard cells but also clusters with an odd number of guard cells that are laterally aligned. The *four lips* mutant, its paralog *myb88*, and the mutant *fama* belong to this group (Yang and Sack, 1995; Bergmann, 2004; Lai et al., 2005). Stomata clusters in GFP-AtMPB2C-overexpressing plants resemble the stomata clusters observed in the first group of mutants, because stomata are arranged at various angles and unpaired guard cells have never been observed.

For mutants of the first group, mutations reside within proteins that are all putative signaling components thought to be involved in the spacing of guard mother cells, an early event in the process of stomata patterning (Bergmann and Sack, 2007). TMM, ER, ERL1, and ERL2 encode Leu-rich repeat-containing receptor-like proteins, whereas SDD1 is a putative subtilisin-related extracellular protease that might be involved in generating an extracellular signal (Nadeau and Sack, 2002; Von Groll et al., 2002). YODA encodes a mitogen-activated kinase kinase kinase. For the second group, all mutated proteins correspond to transcription factors involved in the terminal differentiation step from guard mother cell to guard cell. Because stomata clustering in GFP-AtMPB2C overexpression plants resembles phenotypically the clusters observed in the first group, endogenous AtMPB2C might potentially be connected to the signaling pathway involved in spacing of stomata. So far, none of the proteins connected to stomata spacing has shown an obvious link to the plant cytoskeleton. Thus, AtMPB2C might introduce a novel facet to this process.

Guard cells control gas exchange and transpiration. Plants adjust water loss under changing environmental conditions by regulating opening and closing of stomata. Interestingly, AtMPB2C overexpressors have an increased number of stomata but are resistant toward drought periods. A rapid closure of guard cells in response to water shortage might account for the improved tolerance in plants overexpressing AtMPB2C. Alternatively, guard cells might be generally more closed than in wild-type plants, which might

also contribute to the dwarf phenotype by a possible reduction of carbon assimilation.

Stomatal aperture is regulated by changes in cytoskeletal organization (Hetherington, 2001). Disruption of microtubular function impairs environmentally induced guard cell movement (Fukuda et al., 1998; Marcus et al., 2001). In this respect, it is interesting that AtMPB2C associates with microtubules and overexpression of GFP-AtMPB2C influences the function of cortical microtubules.

Bioinformatic analysis of the three studied MPB2C proteins AtMPB2C, NtMPB2C, and NbMPB2C revealed four conserved patterns, two of which are located within a large predicted coiled-coil region. In addition, there is considerable overall identity of 41% or 44% between AtMPB2C and NtMPB2C or NbMPB2C, respectively, indicating that these proteins likely perform related endogenous functions. It was therefore predicted, based on transient expression experiments with *N. tabacum* MPB2C (Kragler et al., 2003; Curin et al., 2007), that overexpression of AtMPB2C in plants might have a negative effect on viral infectivity. Indeed, analysis of the time course of viral infection revealed that GFP-AtMPB2C-overexpressing plants show increased resistance against ORMV when compared to Arabidopsis wild-type plants. Potentially, upon infection of plants with ORMV, GFP-AtMPB2C might mediate accumulation of ORMV-MP at microtubules, thereby withdrawing the MP from the cell-to-cell transport pathway, similar to the effect observed for NtMPB2C and TMV-MP (Kragler et al., 2003; Curin et al., 2007). In a wild-type situation, part of ORMV-MP is still available to move viral RNA to and through plasmodesmata leading to infection of healthy neighboring cells. In GFP-AtMPB2C-overexpressing plants, less ORMV-MP might be available to promote transport of ORMV RNA into neighboring cells, thereby leading to a decrease in infection efficiency. Interestingly, GFP-AtMPB2C-overexpressing plants infected with LS-CMV showed a similar infection rate as Arabidopsis wild-type plants, indicating that GFP-AtMPB2C-overexpressing plants are not generally more resistant to plant viruses but that the interaction between GFP-AtMPB2C and ORMV-MP is specific. At present, the tools to directly test this model are not available.

MATERIALS AND METHODS

Alignment and Sequence Analysis of MPB2C Proteins

The T Coffee server (http://tcoffee.vital-it.ch/cgi-bin/Tcoffee/tcoffee_cgi/index.cgi; Notredame et al., 2000; Poirot et al., 2003) was used to align AtMPB2C, NtMPB2C, and NbMPB2C protein sequences. The resulting output in Clustal format was submitted to http://bioweb.pasteur.fr/seqanal/interfaces/boxshade.html, a server that was used to shade the multiple-aligned MPB2C sequences. Conserved patterns in MPB2C protein sequences were detected by PRATT (http://www.ebi.ac.uk/pratt). Four conserved patterns were found. Coiled coil domains were detected by Pepcoil (http://bioweb.pasteur.fr/seqanal/interfaces/pepcoil.html).

Generation of Binary Construct pMDC43-GFP-AtMPB2C

Total RNA of Arabidopsis (*Arabidopsis thaliana*) Col-0 leaf tissue was extracted using the RNeasy Plant Mini kit (Qiagen) according to the manufacturer's instructions. Reverse transcription of the AtMPB2C mRNA was performed according to the following conditions: 10 μL of total RNA (1 μg) was incubated at 65°C for 5 min to destroy RNA secondary structures, placed on ice, and mixed with 10 μL of reaction mixture containing 1 mM dNTPs, 5× AMV Reverse Transcription buffer (Promega), 2.5 units of AMV Reverse Transcriptase (Promega), 20 mM dithiothreitol, 40 units RNAsin (Promega), and 5 pmol of primer revAtMPB2C-TOPO (5′-TTAATATGTAAAGGCTAGTGATTGCAGG-3′). The reaction mixture was incubated for 2 h at 42°C. AtMPB2C cDNA was amplified by PCR by adding primers AtMPB2C-TOPO (5′-CACCATGTATGAGCAGCAGCAACATTTC-3′) and revAtMPB2C-TOPO (5′-TTAATATGTAAAGGCTAGTGATTGCAGG-3′) with the following PCR conditions: 5 min at 95°C, followed by 40 cycles consisting of 30 s at 95°C, 1 min 45 s at 55°C, and 1 min at 72°C, followed by 7 min at 72°C. Primer AtMPB2C-TOPO was chosen such that the PCR fragment encoding the AtMPB2C cDNA could be cloned directionally into the pENTR/D-TOPO vector, a Gateway entry vector specifically designed for directional cloning (Invitrogen). Cloning was done according to the protocol of the manufacturer, giving rise to vector pENTR/D-AtMPB2C. The sequence of the 981-bp AtMPB2C cDNA was confirmed by sequencing.

The T-DNA transformation vector pMDC43 (Curtis and Grossniklaus, 2003) contains two 35S cauliflower mosaic virus promoters followed by a GFP coding sequence and a hygromycin resistance gene. The AtMPB2C cDNA from pENTR/D-AtMPB2C was inserted 3′ of the GFP coding sequence into vector pMDC43 by an in vitro LR recombination reaction performed according to the protocol of the manufacturer (Invitrogen), thereby giving rise to the construct pMDC43-GFP-AtMPB2C.

Biolistic Bombardment Procedure

For biolistic delivery, a hand-held gene gun (Bio-Rad Laboratories) was used. A total of 25 μg of plasmid pMDC43-GFP-AtMPB2C was coated onto 12.5 mg of 1-μm gold particles according to the manufacturer's instructions (Bio-Rad Laboratories). Arabidopsis leaves were bombarded at the bottom side of rosette leaves with a helium pressure of 250 psi (Trutnyeva et al., 2008). Expressing cells were analyzed by confocal microscopy 24 h after bombardment.

Confocal Microscopy and Image Processing

A small piece of plant tissue was excised and analyzed with a TCS-SP confocal microscope (Leica Microsystems). GFP fluorescence was excited with an ArKr laser at 488 nm and detected at 500 to 550 nm. Serial optical sections were acquired in 1-μm steps. These sections were then assembled into projections using software supplied by the manufacturer (Leica Microsystems).

Generation of GFP-AtMPB2C-Overexpressing Arabidopsis Plants

The pMDC43-GFP-AtMPB2C vector was transformed into Arabidopsis Col-0 plants using Agrobacteria strain GV3101 (Clough and Bent, 1998). Seeds were collected and grown on selective GM medium (4.3 g Murashige and Skoog basal salt mixture [Sigma-Aldrich], 10 g Suc, 0.5 g MES [Sigma-Aldrich], 8 g agar, 1× vitamins of Murashige and Skoog vitamin powder [Sigma-Aldrich], pH 6.0) containing 20 μg mL^{-1} hygromycin. Nonsegregating plant lines were established and used for all experiments.

Plant Material and Growth Conditions

Arabidopsis Col-0 stably overexpressing MAP4-GFP (Marc et al., 1998; Granger and Cyr, 2001) or Arabidopsis *gl1* stably overexpressing GFP-TUA6 were used (Ueda et al., 1999). For evaluation of phenotype for seed production, Arabidopsis plants were grown on GM medium or on soil at 22°C under long-day conditions (16 h light/8 h dark). Plants for viral infections were grown on soil at 22°C under short-day conditions (8 h light/16 h dark). *Nicotiana tabacum* plants were grown on soil at 20°C under long-day conditions (16 h light/8 h dark).

Western Blot for Detection of GFP-AtMPB2C Fusion Protein

Arabidopsis leaf tissue was frozen and ground to powder in liquid nitrogen. Proteins were extracted by shaking the powder in the same volume of 2× Laemmli sample buffer for 30 min and subsequent boiling for 10 min. The extract was cleared by ultracentrifugation at 35,000*g* for 1 h. Proteins were separated on 12% SDS-PAGE gels and blotted onto nitrocellulose membrane. The blot was blocked in M-TBS (5% [w/v] milk powder, 10 mM Tris-HCl, pH 7.5, and 150 mM sodium chloride) for 30 min, incubated for 2 h with anti-GFP antibody (Roche) at a dilution of 1:1,000 in M-TBS, washed three times with M-TBS, and incubated for 1 h with alkaline phosphatase-coupled goat anti-mouse antibody (Sigma-Aldrich) diluted at 1:30,000 in M-TBS. After washing three times with M-TBS and once with TBS (10 mM Tris-HCl, pH 7.5, and 150 mM sodium chloride), the blot was developed with nitroblue tetrazolium chloride and 5-bromo-4-chloro-3-indolyl-phosphate.

Analysis of Sensitivity of Arabidopsis Wild-Type Plants and GFP-AtMPB2C-Overexpressing Plants to Drought

Thirty plants of each line, Arabidopsis wild-type and GFP-AtMPB2C overexpressor plants, were germinated on 0.5× Murashige and Skoog medium and transferred to soil in single pots 10 d after germination. Plants were grown under long-day conditions. For drought stress, 4-week-old plants were withheld from water for 2 weeks. The survival rate was determined after 48 h of rehydration of wilted plants.

Preparation of ORMV Particles from *N. tabacum*

Six-week-old *N. tabacum* plants were mechanically inoculated with ORMV particles. Plants were regularly visually inspected for mosaic symptoms and necrotic lesions, which became apparent 3 weeks after inoculation. Purification of ORMV particles was done from 20 g of symptomatic leaves, similar to that of TMV particles (Chapman, 1998). The concentration of the viral particles was determined by measuring the A_{260}. The yield was estimated assuming an extinction coefficient of 3.0 for a 1 mg mL^{-1} solution.

Purification of LS-CMV Virions

All steps were performed with autoclaved material at 4°C or on ice. LS-CMV-infected *N. tabacum* tissue was homogenized by grinding in 1 mL buffer A (0.5 M sodium citrate, pH 5.7) per gram of plant tissue. One volume of chloroform and 0.1% of total volume of thioglycolic acid was added. The homogenized plant tissue was centrifuged at 11,950*g* for 10 min. The upper, aqueous phase was filtered through Miracloth, pipetted onto a 10% Suc cushion, and centrifuged at 185,500*g* in an ultracentrifuge for 90 min. The virion pellet was resuspended in 3 mL buffer C (0.05 M sodium citrate, pH 7.0) overnight and cleared by centrifugation at 5,400*g* for 10 min. Three parts of supernatant were mixed with 1 part of 10% Suc cushion and centrifuged in an ultracentrifuge at 48,500*g* for 90 min. The virion pellet was resuspended in 1 mL buffer C overnight, and a final centrifugation at 5,400*g* for 10 min was performed. Virion concentration was determined at 260 nm. $OD_{260} = 5$ for 1 mg mL^{-1} LS-CMV.

Purification of Viral LS-CMV RNA

Virion solution was mixed with 1 volume VEBA (0.2 M Tris, pH 8.5, 1 M NaCl, 2 mM EDTA, 1% SDS), 1 volume chloroform, and 4 volumes phenol, stirred at room temperature for 15 min, and centrifuged at 11,950*g* for 10 min at room temperature. The upper, aqueous phase was recovered, and the procedure was repeated once with 1 volume chloroform and 2 volumes phenol and a second time with 0.2 volumes chloroform and 0.8 volumes phenol, followed by centrifugation at 11,950*g* for 10 min at 4°C. Next, the upper, aqueous phase was recovered, mixed with 1 volume 1-butanol, and centrifuged at 2,900*g* for 5 min at 4°C. The upper 1-butanol phase was discarded. To precipitate RNA, the aqueous phase was mixed with 2.5 volumes absolute ethanol and 0.1 volume 2 M sodium acetate, pH 5.2, incubated for at least 3 h at 4°C and centrifuged at 7,650*g* for 20 min at 4°C. The RNA pellet was washed with 70% ethanol, air dried for 10 min, and dissolved in an appropriate amount of water. RNA concentration was determined by measuring A_{260}.

Analysis of ORMV and LS-CMV Infectivity of Arabidopsis Wild-Type Plants and GFP-AtMPB2C-Overexpressing Plants

Purified ORMV particles at a concentration of 40 ng μL^{-1} in 50 mM phosphate buffer (0.5 M disodium hydrogen orthophosphate, pH 7.2) served as standardized inoculum for infection. Three leaves per plant were dusted with silicon carbide powder and 5 μL of diluted ORMV particle solution was rubbed into the surface of each leaf. At 3, 5, 7, and 14 d postinoculation, the green tissue of 10 Arabidopsis plants and 10 GFP-AtMPB2C-overexpressing plants, respectively, was individually frozen in liquid nitrogen. Similarly, wild-type plants and GFP-AtMPB2C-overexpressing plants were inoculated with 0.5 μg of purified LS-CMV RNA per plant. Green tissue was harvested at 3, 7, 10, and 14 d postinoculation. Plants were homogenized individually in 2× Laemmli sample buffer, and total protein extract was prepared by shaking for 30 min and boiled for 10 min at 95°C. Proteins were separated on a 12% denaturing SDS-PAGE gel and stained with Coomassie Brilliant Blue R-250. Plants were scored positive for infection if a coat protein band was visible. The percentage of infected plants for each time point and plant line was calculated and the weighted mean of the percentage of infection and the error of the weighted mean were calculated and assembled into a graph (Trutnyeva et al., 2005). For each virus, 120 wild type and 120 GFP-AtMPB2C-overexpressing plants were evaluated.

Depolymerization of Microtubules with Oryzalin

Oryzalin (Sigma-Aldrich) was used at a concentration of 20 μM in 0.1% ethanol. Leaves of GFP-AtMPB2C-overexpressing plants and GFP-TUA6-overexpressing plants were cut into pieces and incubated at room temperature in 20 μM oryzalin or in 0.1% ethanol for 20 h.

Phenotypic Analysis of Stomata Pattern

To remove chlorophyll, plant tissue was repeatedly washed in 70% ethanol until the ethanol remained clear. Washing was continued in 40, 20, and 10% ethanol for 5 to 10 min each, followed by incubation in 4% ethanol and 25% glycerol for 2 h or overnight. For staining, the leaves were washed twice with water and incubated for 30 min in a 20-μg/mL propidium iodide solution (Sigma-Aldrich). Plant tissue was mounted on a microscope slide and examined on the abaxial side of leaves with a Leica TCS-SP confocal microscope (Leica Microsystems). Propidium iodide fluorescence was excited at 488 nm and detected at 600 to 620 nm. Four images were taken per leaf. Twelve leaves of GFP-AtMPB2C-overexpressing plants and 12 leaves of Arabidopsis wild-type plants grown on GM medium were analyzed by counting the total number of stomata. The percentage of stomata in clusters was determined.

ACKNOWLEDGMENTS

We thank Fernando Ponz and Carmen Mansilla for providing ORMV-infected material, Fernando García-Arenal for LS-CMV-infected material, and Takashi Hashimoto for the gift of GFP-TUA6 transgenic seeds. We also thank Marie-Theres Hauser for providing MAP4-GFP transgenic seeds.

Received September 26, 2008; accepted November 25, 2008; published December 12, 2008.

LITERATURE CITED

Abe T, Hashimoto T (2005) Altered microtubule dynamics by expression of modified alpha-tubulin protein causes right-handed helical growth in transgenic Arabidopsis plants. Plant J **43:** 191–204

Aguilar I, Sánchez F, Martín AM, Martínez-Herrera D, Ponz F (1996) Nucleotide sequence of Chinese rape mosaic virus (oilseed rape mosaic virus), a crucifer tobamovirus infectious on *Arabidopsis thaliana*. Plant Mol Biol **30:** 191–197

Ambrose JC, Shoji T, Kotzer AM, Pighin JA, Wasteneys GO (2007) The *Arabidopsis* CLASP gene encodes a microtubule-associated protein involved in cell expansion and division. Plant Cell **19:** 2763–2775

Ashby J, Boutant E, Seemanpillai M, Groner A, Sambade A, Ritzenthaler

C, Heinlein M (2006) Tobacco mosaic virus movement protein functions as a structural microtubule-associated protein. J Virol **80:** 8329–8344

Bergmann DC (2004) Integrating signals in stomatal development. Curr Opin Plant Biol **7:** 26–32

Bergmann DC, Sack FD (2007) Stomatal development. Annu Rev Plant Biol **58:** 163–181

Boyko V, Hu Q, Seemanpillai M, Ashby J, Heinlein M (2007) Validation of microtubule-associated Tobacco mosaic virus RNA movement and involvement of microtubule-aligned particle trafficking. Plant J **51:** 589–603

Brandner K, Sambade A, Boutant E, Didier P, Mely Y, Ritzenthaler C, Heinlein M (2008) Tobacco mosaic virus movement protein interacts with green fluorescent protein-tagged microtubule end-binding protein 1. Plant Physiol **147:** 611–623

Buschmann H, Fabri CO, Hauptmann M, Hutzler P, Laux T, Lloyd CW, Schaffner AR (2004) Helical growth of the Arabidopsis mutant tortifolia1 reveals a plant-specific microtubule-associated protein. Curr Biol **14:** 1515–1521

Chapman NS (1998) Tobamovirus isolation and RNA extraction. *In* GD Foster, SC Taylor, eds, Methods in Molecular Biology, Vol 81. Humana Press, Totowa, NJ, pp 123–129

Clough SJ, Bent AF (1998) Floral dip: a simplified method for *Agrobacterium*-mediated transformation of *Arabidopsis thaliana*. Plant J **16:** 735–743

Curin M, Ojangu EL, Trutnyeva K, Ilau B, Truve E, Waigmann E (2007) MPB2C, a microtubule-associated plant factor, is required for microtubular accumulation of tobacco mosaic virus movement protein in plants. Plant Physiol **143:** 801–811

Curtis MD, Grossniklaus U (2003) A gateway cloning vector set for high-throughput functional analysis of genes in planta. Plant Physiol **133:** 462–469

Fukuda M, Hasezawa S, Asai N, Nakajima N, Kondo N (1998) Dynamic organization of microtubules in guard cells of Vicia faba L. with diurnal cycle. Plant Cell Physiol **39:** 80–86

Granger CL, Cyr RJ (2001) Spatiotemporal relationships between growth and microtubule orientation as revealed in living root cells of Arabidopsis thaliana transformed with green-fluorescent-protein gene construct GFP-MBD. Protoplasma **216:** 201–214

Hashimoto T (2002) Molecular genetic analysis of left-right handedness in plants. Philos Trans R Soc Lond B Biol Sci **357:** 799–808

Heinlein M (2002) The spread of tobacco mosaic virus infection: insights into the cellular mechanism of RNA transport. Cell Mol Life Sci **59:** 58–82

Hetherington AM (2001) Guard cell signaling. Cell **107:** 711–714

Hofmann C, Sambade A, Heinlein M (2007) Plasmodesmata and intercellular transport of viral RNA. Biochem Soc Trans **35:** 142–145

Hugdahl JD, Morejohn LC (1993) Rapid and reversible high-affinity binding of the dinitroaniline herbicide oryzalin to tubulin from *Zea mays* L. Plant Physiol **102:** 725–740

Ishida T, Kaneko Y, Iwano M, Hashimoto T (2007) Helical microtubule arrays in a collection of twisting tubulin mutants of Arabidopsis thaliana. Proc Natl Acad Sci USA **104:** 8544–8549

Kawamura E, Himmelspach R, Rashbrooke MC, Whittington AT, Gale KR, Collings DA, Wasteneys GO (2006) MICROTUBULE ORGANIZATION 1 regulates structure and function of microtubule arrays during mitosis and cytokinesis in the Arabidopsis root. Plant Physiol **140:** 102–114

Korolev AV, Buschmann H, Doonan JH, Lloyd CW (2007) AtMAP70-5, a divergent member of the MAP70 family of microtubule-associated proteins, is required for anisotropic cell growth in Arabidopsis. J Cell Sci **120:** 2241–2247

Kragler F, Curin M, Trutnyeva K, Gansch A, Waigmann E (2003) MPB2C, a microtubule-associated plant protein binds to and interferes with cell-to-cell transport of tobacco mosaic virus movement protein. Plant Physiol **132:** 1870–1883

Lai LB, Nadeau JA, Lucas J, Lee EK, Nakagawa T, Zhao L, Geisler M, Sack FD (2005) The *Arabidopsis* R2R3 MYB proteins FOUR LIPS and MYB88 restrict divisions late in the stomatal cell lineage. Plant Cell **17:** 2754–2767

Liu JZ, Blancaflor EB, Nelson RS (2005) The tobacco mosaic virus 126-kilodalton protein, a constituent of the virus replication complex, alone or within the complex aligns with and traffics along microfilaments. Plant Physiol **138:** 1853–1865

Lucas WJ (2006) Plant viral movement proteins: agents for cell-to-cell trafficking of viral genomes. Virology **344:** 169–184

Lupas A, Van Dyke M, Stock J (1991) Predicting coiled coils from protein sequences. Science **252:** 1162–1164

Marc J, Granger CL, Brincat J, Fisher DD, Kao T, McCubbin AG, Cyr RJ (1998) A GFP-MAP4 reporter gene for visualizing cortical microtubule rearrangements in living epidermal cells. Plant Cell **10:** 1927–1940

Marcus AI, Moore RC, Cyr RJ (2001) The role of microtubules in guard cell function. Plant Physiol **125:** 387–395

Martín AM, Martínez-Herrera D, Poch H, Ponz F (1997) Variability in the interactions between *Arabidopsis thaliana* ecotypes and oilseed rape mosaic tobamovirus. Aust J Plant Physiol **24:** 275–281

Nadeau JA, Sack FD (2002) Control of stomatal distribution on the Arabidopsis leaf surface. Science **296:** 1697–1700

Notredame C, Higgins DG, Heringa J (2000) T-Coffee: a novel method for fast and accurate multiple sequence alignment. J Mol Biol **302:** 205–217

Olson KR, McIntosh JR, Olmsted JB (1995) Analysis of MAP 4 function in living cells using green fluorescent protein (GFP) chimeras. J Cell Biol **130:** 639–650

Pierre P, Pepperkok R, Kreis TE (1994) Molecular characterization of two functional domains of CLIP-170 in vivo. J Cell Sci **107:** 1909–1920

Poirot O, O'Toole E, Notredame C (2003) Tcoffee@igs: a web server for computing, evaluating and combining multiple sequence alignments. Nucleic Acids Res **31:** 3503–3506

Roossinck MJ, Zhang L, Hellwald KH (1999) Rearrangements in the 5′ nontranslated region and phylogenetic analyses of cucumber mosaic virus RNA 3 indicate radial evolution of three subgroups. J Virol **73:** 6752–6758

Sedbrook JC (2004) MAPs in plant cells: delineating microtubule growth dynamics and organization. Curr Opin Plant Biol **7:** 632–640

Shoji T, Narita NN, Hayashi K, Asada J, Hamada T, Sonobe S, Nakajima K, Hashimoto T (2004) Plant-specific microtubule-associated protein SPIRAL2 is required for anisotropic growth in Arabidopsis. Plant Physiol **136:** 3933–3944

Shpak ED, McAbee JM, Pillitteri LJ, Torii KU (2005) Stomatal patterning and differentiation by synergistic interactions of receptor kinases. Science **309:** 290–293

Thitamadee S, Tuchihara K, Hashimoto T (2002) Microtubule basis for left-handed helical growth in Arabidopsis. Nature **417:** 193–196

Trutnyeva K, Bachmaier R, Waigmann E (2005) Mimicking carboxyterminal phosphorylation differentially effects subcellular distribution and cell-to-cell movement of tobacco mosaic virus movement protein. Virology **332:** 563–577

Trutnyeva K, Ruggenthaler P, Waigmann E (2008) Movement profiles, a tool for quantitative analysis of cell-to-cell movement of plant viral movement proteins. *In* GD Foster, IE Johansen, Y Hong, PD Nagy, eds, From Viral Sequence to Protein Function, Vol 2. Humana Press, Totowa, NJ, pp 317–330

Ueda K, Matsuyama T, Hashimoto T (1999) Visualization of microtubules in living cells of transgenic *Arabidopsis thaliana*. Protoplasma **206:** 201–206

Von Groll U, Berger D, Altmann T (2002) The subtilisin-like serine protease SDD1 mediates cell-to-cell signaling during *Arabidopsis* stomatal development. Plant Cell **14:** 1527–1539

Waigmann E, Ueki S, Trutnyeva K, Citovsky V (2004) The ins and outs of non-destructive cell-to-cell and systemic movement of plant viruses. Crit Rev Plant Sci **23:** 195–250

Wasteneys GO (2004) Progress in understanding the role of microtubules in plant cells. Curr Opin Plant Biol **7:** 651–660

Whittington AT, Vugrek O, Wei KJ, Hasenbein NG, Sugimoto K, Rashbrooke MC, Wasteneys GO (2001) MOR1 is essential for organizing cortical microtubules in plants. Nature **411:** 610–613

Winter N, Kollwig G, Zhang S, Kragler F (2007) MPB2C, a microtubule-associated protein, regulates non-cell-autonomy of the homeodomain protein KNOTTED1. Plant Cell **19:** 3001–3018

Wright KM, Wood NT, Roberts AG, Chapman S, Boevink P, Mackenzie KM, Oparka KJ (2007) Targeting of TMV movement protein to plasmodesmata requires the actin/ER network: evidence from FRAP. Traffic **8:** 21–31

Yang M, Sack FD (1995) The too many mouths and four lips mutations affect stomatal production in *Arabidopsis*. Plant Cell **7:** 2227–2239

Yuen CY, Pearlman RS, Silo-Suh L, Hilson P, Carroll KL, Masson PH (2003) WVD2 and WDL1 modulate helical organ growth and anisotropic cell expansion in Arabidopsis. Plant Physiol **131:** 493–506